

Highly Anisotropic g -Factor of Two-Dimensional Hole Systems

R. Winkler

Institut für Technische Physik III, Universität Erlangen-Nürnberg, Staudtstrasse 7, D-91058 Erlangen, Germany

S. J. Papadakis, E. P. De Poortere, and M. Shayegan

Department of Electrical Engineering, Princeton University, Princeton, New Jersey 08544

(Received 10 April 2000)

Coupling the spin degree of freedom to the anisotropic orbital motion of two-dimensional (2D) hole systems gives rise to a highly anisotropic Zeeman splitting with respect to different orientations of an in-plane magnetic field \mathbf{B} relative to the crystal axes. This mechanism has no analog in the bulk band structure. We obtain good, qualitative agreement between theory and experimental data, taken in GaAs 2D hole systems grown on (113) substrates, showing the anisotropic depopulation of the upper spin subband as a function of in-plane \mathbf{B} .

PACS numbers: 71.70.Ej, 73.20.Dx

Since the early days of two-dimensional (2D) carrier systems in semiconductors it has been commonly assumed that the Zeeman energy splitting, $\Delta E = g^* \mu_B B$, with g^* the effective g factor and μ_B the Bohr magneton, is independent of the direction of the external magnetic field B [1]. Recently, however, calculations and experiments have shown that g^* can have different values for \mathbf{B} applied in the direction normal to the plane of the 2D system compared to in-plane [2–6]. Here we report calculations and experimental data for 2D holes occupying the heavy hole subband, demonstrating that, even for a purely in-plane \mathbf{B} , g^* can depend strongly on the orientation of \mathbf{B} with respect to the crystal axes [7].

In bulk semiconductors the motion of electrons and holes in the presence of spin-orbit interaction gives rise to a g^* which is significantly modified compared to the free particle g factor $g_0 = 2$ (Ref. [8]). The resulting g^* of holes (and electrons) is nearly isotropic. Commonly, the isotropic part of the hole g^* is denoted by κ [9]. The anisotropic part, q , is typically 2 orders of magnitude smaller than κ and, in the present discussion, is neglected completely. The smallness of q is in sharp contrast to the orbital motion of holes for which we have highly anisotropic effective masses m^* reflecting the spatial anisotropy of the crystal structure. In a 2D hole system (2DHS) we have heavy hole (HH) subbands (z component of angular momentum $M = \pm 3/2$) and light hole (LH) subbands ($M = \pm 1/2$). In the presence of an in-plane \mathbf{B} , κ couples the two LH states, and the HH states to the LH states [4]. But there is no direct coupling between the HH states proportional to κ . Therefore, the authors of Refs. [3–6] concluded that the Zeeman splitting of HH states due to an in-plane \mathbf{B} is suppressed. From a group-theoretical point of view, the in-plane/out-of-plane anisotropy discussed in Refs. [2–6] can be traced back to the fact that, apart from the small terms dependent on q and wave vector \mathbf{k} , the bulk Zeeman Hamiltonian [8,9] has spherical symmetry which in 2D systems is reduced to an axial symmetry. However, due to the anisotropic orbital motion, the symmetry of the

total Hamiltonian is lower than axial. Thus for crystallographic directions other than the high-symmetry directions [001] and [111] (neglecting a broken inversion symmetry) and nonzero spin-orbit interaction it follows that g^* can depend on the direction of the in-plane \mathbf{B} . Here we will show that, in agreement with these symmetry considerations, a new mechanism gives rise to a large and highly anisotropic Zeeman splitting with respect to different orientations of the in-plane magnetic field \mathbf{B} relative to the crystal axes.

In the following we will discuss quantum wells (QW's) grown in the crystallographic $[mmn]$ direction (with m, n integers). Hence we use the coordinate system shown in Fig. 1(a) with θ denoting the angle between $[mmn]$ and [001]. We remark that recently QW's for 2DHS's have often been grown in [113] direction as this yields particularly high hole mobilities [10].

In general, the dynamics of 2D holes is rather complicated due to the nonparabolic and anisotropic terms in the Hamiltonian. Therefore, a quantitative understanding of

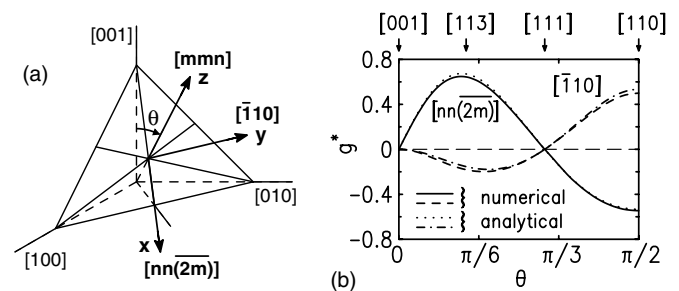


FIG. 1. (a) Coordinate system for QW's grown in $[mmn]$ direction (z direction). Here θ is the angle between $[mmn]$ and [001], i.e., we have $\theta = \arccos(n/\sqrt{2m^2 + n^2})$. The axes for the in-plane motion are $[nn(2m)]$ (x) and $[\bar{1}10]$ (y). (b) Anisotropic effective g factor g^* of the HH1 subband for a 200 Å wide GaAs/Al_{0.3}Ga_{0.7}As QW as a function of the angle θ . Results are shown for the in-plane \mathbf{B} along the $[nn(2m)]$ and $[\bar{1}10]$ directions. The solid and dashed lines were obtained by means of a numerical diagonalization of the Luttinger Hamiltonian. The dotted and dash-dotted lines were obtained by means of Eq. (1).

phenomena such as the anisotropic Zeeman splitting can be obtained only by means of accurate, numerical computations [11]. In particular, the Zeeman splitting of 2D hole states depends on higher orders both of the in-plane wave vector $\mathbf{k}_{\parallel} = (k_x, k_y, 0)$ and of \mathbf{B} . As we will show next, it is, nevertheless, very helpful for a qualitative understanding to identify analytically the relevant lowest order terms.

We describe the hole subband states by means of the 4×4 Luttinger Hamiltonian [9] using a symmetry-adapted basis [12]. The anisotropy of the orbital motion can be characterized by a single parameter $\delta \equiv \gamma_3 - \gamma_2$ (Ref. [13]), where γ_1 (used below), γ_2 , and γ_3 are the Luttinger parameters [9]. For growth directions other than [001] and [111] even at the bottom of the hole subbands, i.e., for $\mathbf{k}_{\parallel} = 0$, the anisotropic motion results in an off-diagonal HH-LH mixing proportional to δk_z^2 which complements the HH-LH coupling proportional to κB . Treating both terms by means of degenerate perturbation theory we obtain in second order for g^* at the bottom of the HH subbands in an infinitely deep rectangular QW

$$g_{[nn(2m)]}^{\text{HH}} = 6[2 - 3 \sin^2(\theta)] \sin(\theta) \sqrt{4 - 3 \sin^2(\theta)} \times \frac{\kappa \delta}{\gamma_z^{\text{HH}} - \gamma_z^{\text{LH}}}, \quad (1a)$$

$$g_{[\bar{1}10]}^{\text{HH}} = -6[2 - 3 \sin^2(\theta)] \sin^2(\theta) \frac{\kappa \delta}{\gamma_z^{\text{HH}} - \gamma_z^{\text{LH}}}, \quad (1b)$$

with

$$\gamma_z^{\text{HH}} = -\gamma_1 + 2[(1 - \alpha)\gamma_2 + \alpha\gamma_3], \quad (2a)$$

$$\gamma_z^{\text{LH}} = -\gamma_1 - 2[(1 - \alpha)\gamma_2 + \alpha\gamma_3], \quad (2b)$$

$$\alpha = \sin^2(\theta) [3 - \frac{9}{4} \sin^2(\theta)]. \quad (2c)$$

Here γ_z^{HH} and γ_z^{LH} are the reciprocal effective masses in z direction in the axial approximation for the HH and LH subbands, respectively [12,14]. The anisotropic g factor (1) is proportional to κ and δ , i.e., it is due to the *combined* effect of the isotropic bulk Zeeman Hamiltonian and the anisotropic orbital motion in the valence band. It disappears in the axial limit $\delta = 0$. Equation (1) has no analog in the bulk band structure [8,9]. Moreover, it is fundamentally different from the anisotropic g^* discussed in Refs. [2–6]. Our sign convention for g^* used in Eq. (1) corresponds to the dominant spinor component of the multicomponent eigenstates (using a basis of angular momentum eigenfunctions with quantization axis in the direction of \mathbf{B}). We remark that in unstrained QW's the topmost subband is the HH1 subband.

For LH subbands in an in-plane \mathbf{B} as well as for HH and LH subbands in a perpendicular \mathbf{B} , g^* contains terms similar to Eq. (1). However, the dominant contribution is given by the bulk g factor κ . For LH subbands in an in-plane \mathbf{B} we have basically $g_{\parallel}^{\text{LH}} = 4\kappa$, while for a perpendicular \mathbf{B} we have $g_z^{\text{HH}} = 6\kappa$ and $g_z^{\text{LH}} = 2\kappa$ (Refs. [6,9]).

Yet, this implies a remarkable difference [3–6] compared with Eq. (1).

In Fig. 1(b) we show the anisotropic g^* of the HH1 subband for a 200 Å wide GaAs/Al_{0.3}Ga_{0.7}As QW as a function of the angle θ . The analytical expressions (1) (dotted and dash-dotted lines) are in very good agreement with the more accurate results obtained by means of a numerical diagonalization [4,11] of the Luttinger Hamiltonian (solid and dashed lines). Figure 1(b) demonstrates that g^* can be very anisotropic [15]. For example, for the growth direction [113], g^* is about a factor of 4 larger when $B \parallel [33\bar{2}]$ compared to when $B \parallel [\bar{1}10]$. Moreover, the sign of $g_{[nn(2m)]}^{\text{HH}}$ is opposite to the sign of $g_{[\bar{1}10]}^{\text{HH}}$.

Equation (1) is applicable to a wide range of cubic semiconductors with results qualitatively very similar to Fig. 1(b). In particular, the relative anisotropy

$$\frac{g_{[\bar{1}10]}^{\text{HH}}}{g_{[nn(2m)]}^{\text{HH}}} = -\frac{\sin(\theta)}{\sqrt{4 - 3 \sin^2(\theta)}} \quad (3)$$

is independent of the material-specific parameters γ_i and κ . This remarkable result can be traced back to the fact that the anisotropy for different directions θ in \mathbf{k} space is always characterized by the single parameter δ (Ref. [13]). Note that for QW's based on narrow-gap semiconductors we have a larger κ and smaller effective masses. Thus the absolute values of g^* are significantly larger than g^* of GaAs shown in Fig. 1(b), but the g^* anisotropy is still given by Eq. (3) and depends only on θ . The Zeeman splitting can be even further enhanced if one uses semimagnetic semiconductors containing, e.g., Mn. For these materials the structure of the Hamiltonian is identical to the conventional Luttinger Hamiltonian in the presence of a magnetic field with κ replaced by the effective g factor due to the paramagnetic exchange interaction [5,6]. Therefore Eq. (1) and the g^* anisotropy [Eq. (3)] are readily applicable to semimagnetic materials, also.

In a Taylor expansion of the Zeeman splitting, $\Delta E(B)$, g^* (times μ_B) is the prefactor for the lowest order term linear in B . Often terms of higher order in B are neglected because of their relevant insignificance. An interesting feature of Fig. 1(b) is the vanishing of g^* for the high-symmetry growth directions [001] and [111] (Refs. [4,16]). For the 2DHS discussed in Fig. 1(b) this results in a splitting ΔE which at $B = 1$ T is more than 2 orders of magnitude smaller than ΔE for growth directions [113] and [110]. For these high-symmetry directions ΔE is proportional to B^3 (Ref. [17]). In second order perturbation theory we obtain for the HH1 subband of an infinitely deep rectangular QW of width d grown in [001] direction

$$\Delta E = (\mu_B B)^3 \left(\frac{m_0 d^2}{\pi^2 \hbar^2} \right)^2 \sqrt{\gamma_2^2 \cos^2(2\phi) + \gamma_3^2 \sin^2(2\phi)} \times \left[\frac{4\kappa(\pi^2 - 6)}{\gamma_z^{\text{HH}} - \gamma_z^{\text{LH}}} + \frac{27\gamma_3}{\gamma_z^{\text{HH}} - 9\gamma_z^{\text{LH}}} \right]. \quad (4)$$

Here ϕ is the angle between the in-plane \mathbf{B} and the [100] axis. We get similar, though somewhat longer expressions for growth direction [111]. It is remarkable that we have a nonzero ΔE even in the limit $\kappa = 0$. This can be understood as follows: The 4×4 Luttinger Hamiltonian [9] which is underlying our calculations corresponds to an infinitely large spin-orbit splitting between the topmost valence band Γ_8^v and the split-off band Γ_7^v . Therefore spin-orbit interaction is not explicitly visible in our results, though, similar to Zeeman splitting in bulk semiconductors [8], Eqs. (1) and (4) are a consequence of spin-orbit interaction. In 2D systems the motion of electrons and holes in the presence of this interaction can give rise to a Zeeman splitting even without a bulk g^* . We remark that in a parabolic QW the in-plane g^* of the HH subbands also contains such terms independent of κ . We have here a 2D analog of Roth's famous formula [8] for the electron bulk g^* . Finally we note that, unlike [14] Eq. (1), ΔE in Eq. (4) increases proportional to d^4 , i.e., Zeeman splitting is most efficiently suppressed in narrow QW's.

We have probed the anisotropy of g^* experimentally by measuring the magnetoresistance of a high-mobility 2DHS as a function of in-plane B . The sample is a 200 Å wide Si-modulation doped GaAs QW grown on (113)A GaAs substrate. The left two panels of Fig. 2 show the resistivity ρ measured as a function of in-plane B for three different densities that were changed via back- and front-gate biases.

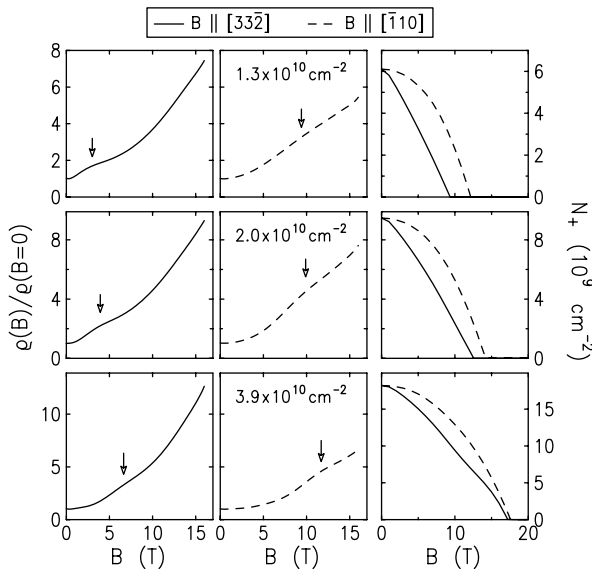


FIG. 2. Left and central panels: Fractional change in resistivity $\rho(B)/\rho(0)$ due to an in-plane B , measured at $T = 0.3$ K in a GaAs 2D hole system grown on a (113) substrate, for \mathbf{B} perpendicular to the current \mathbf{I} and different 2D densities as indicated. Solid lines: $\mathbf{B} \parallel [33\bar{2}]$, dashed lines $\mathbf{B} \parallel [\bar{1}10]$. The arrows mark B^* as defined in the text. The resistivities at $B = 0$ in the left (central) panel are from top to bottom 7.2 (4.9), 2.2 (1.6), and 0.55 (0.45) k Ω /square. Right panel: Calculated density N_+ in the upper spin subband as a function of B . Note that the horizontal axes in the left and central panels and in the right panel have different scales.

The direction of current \mathbf{I} in the measurements of Fig. 2 was kept perpendicular to the direction of in-plane \mathbf{B} . For easier comparison we have plotted the fractional change $\rho(B)/\rho(B = 0)$. Apart from an overall positive magnetoresistance these traces show a broad feature consisting of an inflection point followed by a reduction in slope followed by another inflection point. In Fig. 2 we have placed arrows between the two inflection points at a value of B we call B^* . The magnetoresistance feature at B^* in Fig. 2 is related to a spin-subband depopulation and the resulting changes in subband mobility and intersubband scattering as the in-plane B is increased [18]. It is remarkable that B^* for the $\mathbf{B} \parallel [33\bar{2}]$ traces is several Tesla smaller than for the $[\bar{1}10]$ traces. This is strong evidence for the anisotropy of the in-plane g^* . This interpretation is validated by our self-consistently calculated [4,11,14] results for the density N_+ of the upper spin subband as a function of B , shown in the right panel of Fig. 2. The density N_+ decreases much faster for $\mathbf{B} \parallel [33\bar{2}]$ than for $\mathbf{B} \parallel [\bar{1}10]$, in agreement with Fig. 1(b). Data taken with $\mathbf{I} \parallel \mathbf{B}$ show that while the magnetoresistance changes, B^* is independent of the \mathbf{I} direction and depends only on the density and the direction of \mathbf{B} with respect to crystal axes, therefore supporting the association of B^* with the onset of spin-subband depopulation (see Ref. [18] for more details).

One might ask whether the data in Fig. 2 could be summarized by a single value of g^* for each trace. Unfortunately, this is not possible because, due to the complicated band structure of holes, g^* depends on the in-plane wave vector \mathbf{k}_{\parallel} , and we are averaging over $g^*(\mathbf{k}_{\parallel})$ for \mathbf{k}_{\parallel} up to the Fermi wave vector \mathbf{k}_F . The significance of this effect can be readily deduced from the right panel of Fig. 2, as we would have straight lines for $N_+(B)$ if g^* (and the effective mass m^*) were not dependent on \mathbf{k}_{\parallel} . In Fig. 2 terms of higher order in B are negligibly small.

In Fig. 2 the measured B^* is significantly smaller than the calculated B for a complete depopulation of the upper spin-subband. We note that for our low-density samples it can be expected that g^* is enhanced due to the exchange interaction and the spin polarization caused by the in-plane B [1,19,20]. This effect was not taken into account in our self-consistent calculations. The overall agreement between the experimental data and the calculations, however, implies that these many-particle effects do not qualitatively affect the anisotropy of g^* . We wish to propose that the anisotropic g^* as given in Eq. (1) for in-plane wave vector $\mathbf{k}_{\parallel} = 0$ and without many-body effects may be measured using optical and microwave experiments such as those in Ref. [7].

The large anisotropy of the Zeeman splitting in 2DHS's offers many possible device applications. In a polycrystalline material, e.g., one could alter the degree of spin polarization in different domains by changing the direction of the external \mathbf{B} . As can be seen in Fig. 1(b), because of the sign reversal of g^* it is even possible to have different domains with opposite spin polarization for a given

direction of \mathbf{B} . Recently, there has been a growing interest in controlling the spin degree of freedom for quantum computing and spin electronics. In Ref. [21] the authors have sketched a quantum device which makes use of the spatial variation of g^* in layered semiconductor structures made of, e.g., $\text{Al}_x\text{In}_y\text{Ga}_{1-x-y}\text{As}$. However, the authors have estimated that a substantial change in g^* requires a fairly large electric field of the order of 100 kV/cm. Oestreich *et al.* [22] and Fiederling *et al.* [23] have suggested a spin aligner based on semimagnetic semiconductors. Here the g -factor anisotropy of 2DHS's provides a powerful additional degree of freedom for engineering such devices.

In conclusion, we have shown that coupling the spin degree of freedom to the anisotropic orbital motion of 2D hole systems gives rise to a highly anisotropic Zeeman splitting with respect to different orientations of an in-plane magnetic field relative to the crystal axes.

R.W. wants to thank O. Pankratov and P.T. Coleridge for stimulating discussions and suggestions. Work at Princeton University was supported by the NSF, ARO, and DOE.

-
- [1] F.F. Fang and P.J. Stiles, Phys. Rev. **174**, 823 (1968).
 [2] E. L. Ivchenko and A. A. Kiselev, Sov. Phys. Semicond. **26**, 827 (1992); E. L. Ivchenko, A. A. Kiselev, and M. Willander, Solid State Commun. **102**, 375 (1997). These authors have shown that nonparabolicity leads to a small difference between the electron g^* for a perpendicular and for an in-plane \mathbf{B} . An experimental confirmation of these findings was given, e.g., by B. Kowalski *et al.* [Phys. Rev. B **49**, 14 786 (1994)].
 [3] H. W. van Kesteren *et al.*, Phys. Rev. B **41**, 5283 (1990).
 [4] G. Goldoni and A. Fasolino, Phys. Rev. B **48**, 4948 (1993).
 [5] P. Peyla *et al.*, Phys. Rev. B **47**, 3783 (1993).
 [6] B. Kuhn-Heinrich *et al.*, Solid State Commun. **91**, 413 (1994).
 [7] For electrons in GaAs quantum wells (QW's) a g^* in-plane anisotropy of about 10% was observed experimentally by M. Oestreich, S. Hallstein, and W. W. Rühle [IEEE J. Sel. Top. Quantum Electron. **2**, 747 (1996)]. In a theoretical analysis, V.K. Kalevich and V.L. Korenev [JETP Lett. **57**, 571 (1993)] have argued that the low symmetry C_{2v} of *asymmetric* QW's grown in [001] direction gives rise to an in-plane anisotropy of g^* . However, in their electron Hamiltonian they omitted the Rashba term, which is necessary to obtain the point group C_{2v} ; see, e.g., E. A. de Andrada e Silva, Phys. Rev. B **46**, 1921 (1992). In fact, the g^* anisotropy derived by Kalevich and Korenev disappears after a suitable gauge transformation which shifts the origin of the z axis. This provides a quantitative explanation for the disagreement between experiment and the theory of Kalevich and Korenev, which was noted by Oestreich *et al.*
 [8] L. M. Roth, B. Lax, and S. Zwerdling, Phys. Rev. **114**, 90 (1959).
 [9] J.M. Luttinger, Phys. Rev. **102**, 1030 (1956).
 [10] S. J. Papadakis *et al.*, Science **283**, 2056 (1999).
 [11] R. Winkler and U. Rössler, Phys. Rev. B **48**, 8918 (1993).
 [12] G. Fishman, Phys. Rev. B **52**, 11 132 (1995).
 [13] N.O. Lipari and A. Baldereschi, Phys. Rev. Lett. **25**, 1660 (1970).
 [14] Equation (1) is independent of the well width d . Similar to optical anisotropy in QW's [R. Winkler and A. I. Nesvizhskii, Phys. Rev. B **53**, 9984 (1996); and references therein] g_{\parallel}^* depends on d if the split-off valence band Γ_7^v is explicitly taken into account. Here, we omit the rather lengthy modifications in Eq. (1). They become relevant for narrow QW's with $d \lesssim 50$ Å. The traces in the right panel of Fig. 2 were obtained by means of a more complete 8×8 Hamiltonian containing the bands Γ_6^c , Γ_8^v , and Γ_7^v . However, the results obtained by means of the 4×4 Luttinger Hamiltonian are similar.
 [15] For comparison, we remark that for the GaAs system in Fig. 1(b) we have $g_z^{\text{HH}} = 6\kappa \approx 7.2$.
 [16] The small B -linear Zeeman splitting proportional to q was discussed in Ref. [3]. Note that for a 200 Å wide GaAs QW and magnetic fields $B \gtrsim 3$ T the cubic splitting (4) dominates over the linear splitting due to q . An enhanced B -linear Zeeman splitting of 2D holes is possible in *asymmetric* GaAs QW's [7]. Here we focus on symmetric QW's.
 [17] R. W. Martin *et al.* [Phys. Rev. B **42**, 9237 (1990)] have predicted a Zeeman splitting for growth direction [001] proportional to B^2 . This result was obtained by an incorrect symmetrization of the k dependent terms in the Luttinger Hamiltonian.
 [18] S. J. Papadakis *et al.*, Phys. Rev. Lett. **84**, 5592 (2000).
 [19] Y. Kwon, D.M. Ceperley, and R.M. Martin, Phys. Rev. B **50**, 1684 (1994); and references therein.
 [20] T. Okamoto *et al.*, Phys. Rev. Lett. **82**, 3875 (1999).
 [21] D.P. DiVincenzo *et al.*, in *Quantum Mesoscopic Phenomena and Mesoscopic Devices in Microelectronics*, edited by I. O. Kulik and R. Ellialtioglu, NATO Advanced Study Institute, Vol. 559 (Kluwer Academic Publishers, Boston, 2000).
 [22] M. Oestreich *et al.*, Appl. Phys. Lett. **74**, 1251 (1999).
 [23] R. Fiederling *et al.*, Nature (London) **402**, 787 (1999).